ARTICLES

Photodissociation of Naphthalene Dimer Radical Cation during the Two-Color Two-Laser Flash Photolysis and Pulse Radiolysis−Laser Flash Photolysis

Xichen Cai, Sachiko Tojo, Mamoru Fujitsuka, and Tetsuro Majima*

The Institute of Scientific and Industrial Research (SANKEN), Osaka University, Mihogaoka 8-1, Ibaraki, Osaka 567-0047, Japan

Received: May 3, 2006; In Final Form: June 12, 2006

Photodissociation of naphthalene (Np) dimer radical cation ($Np_2^{\bullet+}$) to give naphthalene radical cation ($Np^{\bullet+}$) and Np and the subsequent regeneration of $Np_2^{\bullet+}$ by the dimerization of $Np^{\bullet+}$ and Np were directly observed during the two-color two-laser flash photolysis in solution at room temperature. When $Np_2^{\bullet+}$ was excited at the charge-resonance (CR) band with the 1064-nm laser, the bleaching and recovery of the transient absorption at 570 and 1000 nm, assigned to the local excitation (LE) and CR bands of $Np_2^{\bullet+}$, respectively, were observed together with the growth and decay of the transient absorption at 685 nm, assigned to $Np^{\bullet+}$. The dissociation of $Np_2^{\bullet+}$ proceeds via a one-photon process within the 5-ns laser flash to give $Np^{\bullet+}$ and Np in the quantum yield of 3.2×10^{-3} and in the chemical yield of 100%. The recovery time profiles of $Np_2^{\bullet+}$ at 570 and 1000 nm were equivalent to the decay time profile of $Np^{\bullet+}$ at 685 nm, suggesting that the dimerization of $Np^{\bullet+}$ and Np occurs to regenerate $Np_2^{\bullet+}$ in 100% yield. Similar experimental results of the photodissociation and regeneration of $Np_2^{\bullet+}$ were observed during the pulse radiolysis-laser flash photolysis of Np in 1,2-dichloroethane. The photodissociation mechanism can be explained based on the crossing between two potential surfaces of the excited-state $Np_2^{\bullet+}$ and ground-state $Np^{\bullet+}$.

Introduction

One-electron oxidation of a variety of aromatic hydrocarbons (ArH) such as benzene, naphthalene (Np), anthracene, and pyrene generates the radical cations ($ArH^{\bullet+}$) which associate partly with the neutral counterparts to form the dimer radical cations ($(ArH)_2^{\bullet+}$) with a $\pi-\pi$ face-to-face structure.[1−9] Because the $(ArH)_2^{\bullet+}$ has a characteristic absorption in the near-IR region, the formation of $(ArH)_2^{\bullet+}$ has been widely studied and used as a powerful probe to monitor the dynamics of macromolecules such as *meso*- and *rac*-2,4-di(*N*-carbazolyl)pentanes, *trans*-1,2-di(*N*-carbazolyl)cyclobutane,[10] poly(3,6-di-*tert*-butyl-9-vinylcarbazole), poly(vinylnaphthalene)s,[11,12] complex [3*n*]-cyclophanes ($n = 3, 5, 6$),[13] oligodeoxynucleotides, and DNA.[7,8,14] For example, the formation of pyrene dimer radical cations has been successfully used to probe the dynamics of DNA in the time scale of microseconds to milliseconds.[7,8] It is notable that the formation of guanine (G) dimer radical cation ($GG^{\bullet+}$) is assumed to be involved in the photooxidative damage of DNA,[15−19] because GG has a lower oxidation potential than G and acts as the hole trapping site. Here we focus on the photodissociation of the naphthalene dimer radical cation ($Np_2^{\bullet+}$).

$Np_2^{\bullet+}$ generated from the dimerization of a naphthalene radical cation ($Np^{\bullet+}$) and Np with a $\pi-\pi$ face-to-face structure has been extensively investigated with experimental and theoretical methods.[5,20−28] $Np_2^{\bullet+}$ has the local excitation (LE) band in the visible region around 570 nm together with the charge resonance (CR) band in the near-IR region around 1000 nm, which originated from the interaction between molecular orbitals of $Np^{\bullet+}$ and Np (Scheme 1).[20−25,27,29]

* Address correspondence to this author. E-mail: majima@sanken.osaka-u.ac.jp. Phone: +81-6-6879-8495. Fax: +81-6-6879-8499.

SCHEME 1: Schematic Diagram of Energy Levels of $Np^{\bullet+}$ and $Np_2^{\bullet+}$ [a]

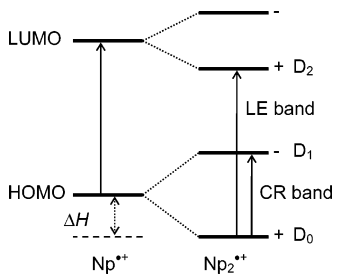

[a] ΔH is the formation enthalpy of $Np_2^{\bullet+}$.

From the electronic interaction between $Np^{\bullet+}$ and Np, the HOMO and LUMO split into two levels (HOMO+, HOMO−, LUMO+, and LUMO−) for $Np_2^{\bullet+}$. The CR and LE bands correspond to the transitions from HOMO+ to HOMO− ($D_1 \leftarrow D_0$) and from HOMO+ to LUMO+ ($D_2 \leftarrow D_0$), respectively. The formation enthalpy ($-\Delta H$) or the stabilization energy of $Np_2^{\bullet+}$ is approximately equal to half of the energy gap between the D_1 and D_0 states (CR band).[27,29] There are two possible conformations for $Np_2^{\bullet+}$, i.e., the partially and fully overlapped conformations. Since the partially overlapped one has a larger $-\Delta H$ value than that of the fully overlapped one,[29,30] the former conformation is preferable for intermolecular $Np_2^{\bullet+}$.[24,27,29,30] Because of the sufficient stabilization energy ($-\Delta H = \sim 50$ kJ mol^{-1}) of $Np_2^{\bullet+}$,[27,31,32] $Np^{\bullet+}$ can exist as $Np_2^{\bullet+}$ in the presence of Np at high concentration. There are many reports on the formation of intra- and intermolecular $Np_2^{\bullet+}$ [12,27,28,31−35] by means of the absorption spectral measurement.[5,20−28]

10.1021/jp062707z CCC: $33.50
Published on Web 07/11/2006

Contrary to the formation of $(ArH)_2^{\bullet+}$, there is no report on the dissociation of $(ArH)_2^{\bullet+}$ in solution, because $(ArH)_2^{\bullet+}$ is thermally more stable than $ArH^{\bullet+}$ in solution. The equilibrium of $(ArH)_2^{\bullet+}$ and $ArH^{\bullet+}$ exists depending on the ArH concentration. The selective thermal activation of $(ArH)_2^{\bullet+}$ with the energy over $-\Delta H$ may cause the dissociation, although it is not possible to be performed in solution. Therefore, the selective photoexcitation of $(ArH)_2^{\bullet+}$ is necessary to study the dissociation of $(ArH)_2^{\bullet+}$. In fact, the photodissociation of Np cluster ions (Np_n^+, $n = 2-7$) has been reported in the gas phase with use of the time-of-flight (TOF) mass analysis method,[27,36,37] although the photodissociation mechanism is not clear. We report here the first example of the photodissociation of $Np_2^{\bullet+}$ to $Np^{\bullet+}$ and Np and the subsequent regeneration of $Np_2^{\bullet+}$ using the two-color two-laser flash photolysis technique[38] and pulse radiolysis−laser flash photolysis combined method in solution at room temperature.[39,40] The photodissociation of $Np_2^{\bullet+}$ occurred to give $Np^{\bullet+}$ and Np within a 5-ns laser flash duration when $Np_2^{\bullet+}$ was excited at the CR band with a 1064-nm 5-ns laser. After the photodissociation, the subsequent regeneration of $Np_2^{\bullet+}$ from the dimerization of $Np^{\bullet+}$ and Np was also observed.

Experimental Section

Materials. Naphthalene was purchased from Nacalai Tesque Inc. and purified from ethanol before use. Chloranil (99%) was purchased from Sigma-Aldrich, Inc. and was used as received. Acetonitrile (spectral grade) and 1,2-dichloroethane (spectral grade) purchased from Nacalai Tesque Inc. were used as received. All sample solutions were freshly prepared before irradiation. All experiments were carried out at room temperature.

Two-Color Two-Laser Flash Photolysis. The 355-nm laser flash from a Nd:YAG laser (Continuum, Surelite II-10; 5-ns full width at half-maximum (fwhm)) was used as the first laser excitation to prepare $Np^{\bullet+}$ and $Np_2^{\bullet+}$. The 1064-nm laser flash (40−180 mJ flash^{-1}) from a Nd:YAG laser (Brilliant, Quantel; 5-ns fwhm) was used as the second laser to excite $Np_2^{\bullet+}$ during the two-color two-laser flash photolysis experiments.[38] Two laser flashes were synchronized by a pulse generator with a delay time of 10 ns−10 μs. The probe beam was obtained from a 450-W Xe-lamp (Osram XBO-450). The transmitted probe beam was focused on a monochromator (Nikon G250). The output of the monochromator was monitored with a photomultiplier tube (PMT, Hamamatsu Photonics R928). The signal from the PMT was recorded on a transient digitizer (Tektronix, TDS 580D). The transient absorption in the near-IR region was monitored with a fast InGaAs PIN photodiode equipped with an amplifier (Thorlabs, PDA255) and the transient digitizer. The total system was controlled with a personal computer via GP−IB interface. To avoid any damage of the sample solution by the probe light, a suitable cutoff filter was used in front of the sample.

Pulse Radiolysis−Laser Flash Photolysis Combined Method. The pulse radiolysis−laser flash photolysis combined method has been described in previous papers.[39,40] Briefly a solution containing Np in 1,2-dichloroethane (DCE) (1.0×10^{-2} M) was irradiated with an electron pulse and sequentially with a laser flash at a delay time of 10 ns to 1 μs after the electron pulse. An electron pulse (28 MeV, 8 ns duration, dose of approximately 0.7 kGy pulse^{-1}, diameter of 0.4 cm) was obtained from a linear accelerator at Osaka University. The 1064-nm laser flash and the signal obtaining system were the same as those used for the two-color two-laser flash photolysis system. The 1064-nm laser flash and the probe beam were synchronized with the electron pulse.

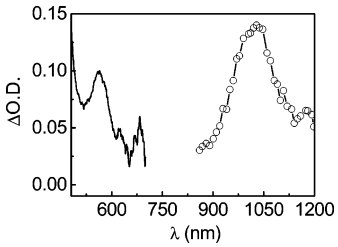

Figure 1. Transient absorption spectrum in the visible (solid line) and near-IR region (solid line plus open circles) observed at 100 ns after the 355-nm laser flash during the 355-nm laser flash photolysis of a mixture of Np (1.0×10^{-2} M) and Chl (5.0×10^{-3} M) in acetonitrile.

Results and Discussion

Formation of $Np^{\bullet+}$ and $Np_2^{\bullet+}$ during the 355-nm Laser Flash Photolysis. When a mixture of Np (1.0×10^{-2} M) and chloranil (Chl) (5.0×10^{-3} M) in acetonitrile was irradiated with the 355-nm laser (6 mJ flash^{-1}) at room temperature, an electron-transfer reaction between Chl in the triplet excited state (^{3}Chl*) and Np occurred to give $Np^{\bullet+}$ and the Chl radical anion ($Chl^{\bullet-}$).[41] Since the Np concentration was enough high, the dimerization of $Np^{\bullet+}$ and Np occurred to give $Np_2^{\bullet+}$.[5,26,30,42]

The transient absorption spectra of $Np^{\bullet+}$ and $Np_2^{\bullet+}$ in the visible and near-IR region were shown in Figure 1. The sharp absorption band with peaks at 625 and 685 nm is assigned to the $D_2 \leftarrow D_0$ transition of $Np^{\bullet+}$.[30,42] No absorption corresponding to the $D_1 \leftarrow D_0$ transition of $Np^{\bullet+}$ was observed because of its dipole-forbidden character, although the theoretical calculation predicts that the transition exists around 1170 nm.[27,36,43,44] The broad absorption bands around 570 and 1000 nm are assigned to the LE and CR bands of $Np_2^{\bullet+}$, respectively.[27,29−32] The transient absorption spectrum of $Chl^{\bullet-}$ has a peak around 450 nm and no significant peak in the region of 500−1200 nm.[41]

The time profiles of the transient absorption at 570, 1000, and 685 nm during the 355-nm irradiation are shown as dotted lines in Figure 2. The formation of $Np^{\bullet+}$ by the electron-transfer reaction between ^{3}Chl* and Np occurred to give $Np^{\bullet+}$ and $Chl^{\bullet-}$, together with the dimerization of $Np^{\bullet+}$ and Np to give $Np_2^{\bullet+}$, in the time scale of 5−50 ns after the 355-nm laser irradiation of the mixture of Np and Chl in acetonitrile. Therefore, the $Np^{\bullet+}$ formation and depletion processes are overlapped in the time scale of 5−100 ns, as shown in Figure 2C (Supporting Information). The growth of the 570- and 1000-nm absorption in the time scale of 5−50 ns was observed and was assigned to the formation of $Np_2^{\bullet+}$ by the dimerization of $Np^{\bullet+}$ and Np as shown in Figure 2A,B. The similar decay profiles of the transient absorption at 570, 1000, and 685 nm in the time scale of a few hundred nanoseconds after the 355-nm laser flash correspond to the charge recombination between $Np_2^{\bullet+}$ or $Np^{\bullet+}$ and $Chl^{\bullet-}$. It has been reported that $Np^{\bullet+}$ is equilibrated with $Np_2^{\bullet+}$ at the equilibrium constant $K = 5.2 \times 10^2$ M^{-1} based on the pulse radiolysis measurements in benzonitrile at 290 K.[5,26,45]

Photodissociation and Regeneration of $Np_2^{\bullet+}$ during the Two-Color Two-Laser Flash Photolysis. When $Np_2^{\bullet+}$ was excited at the CR band with the second 1064-nm laser flash, the bleaching of $Np_2^{\bullet+}$ at 570 ($\Delta\Delta OD_{570}$) and 1000 nm ($\Delta\Delta OD_{1000}$) together with the growth of $Np^{\bullet+}$ at 685 nm ($\Delta\Delta OD_{685}$) were observed within the 5-ns laser flash during the first 355-nm and second 1064-nm laser flash photolysis (Figures 2 and 3). $\Delta\Delta OD_{570}$, $\Delta\Delta OD_{1000}$, and $\Delta\Delta OD_{685}$ increased with the increasing of the second 1064-nm laser power (Figure 4).

When an IR laser is used to irradiate a solution, the IR photon energy converts to the thermal energy to lead the laser-induced

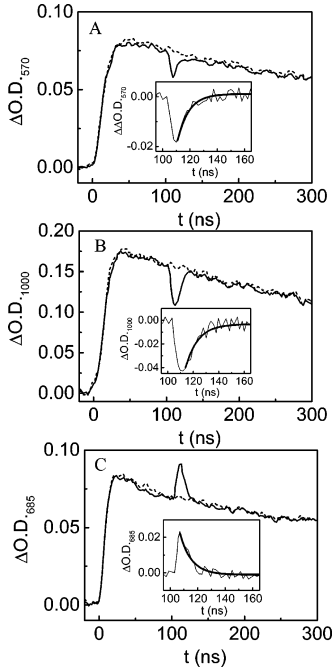

Figure 2. Time profiles of the transient absorption at 570 (A), 1000 (B), and 685 nm (C) assigned to $Np_2^{\bullet+}$, $Np_2^{\bullet+}$, and $Np^{\bullet+}$, respectively, during irradiation of one laser (dotted line) and two lasers with the 1064-nm laser power of 120 mJ flash^{-1} (solid line). The insets show the time profiles of the absorption changes during the second 1064-nm laser irradiation obtained by subtraction of the dotted line from the solid line. The bold solid line in the inset was the fitting curve to the pseudo-first-order exponential function. The delay time of the second 1064-nm laser after the first 355-nm laser was 100 ns.

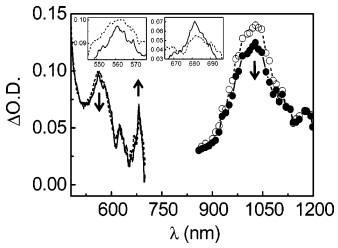

Figure 3. Transient absorption spectra observed at 10 ns after the 1064-nm laser flash during the irradiation of the 355-nm laser (broken line in the visible region and broken line with open circles in the IR region) and two lasers (355- and 1064-nm lasers; solid line in the visible region and solid line plus closed circles in the IR region) with the power of 6 and 120 mJ flash^{-1}, respectively. The insets show the expanded spectra in the regions of 550−580 and 675−690 nm.

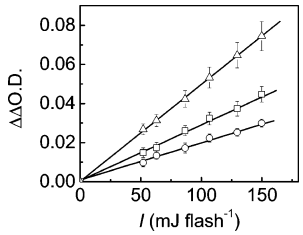

Figure 4. Plots of $\Delta\Delta OD_{570}$ (circles), $\Delta\Delta OD_{1000}$ (triangles), $\Delta\Delta OD_{685}$ (squares) vs 1064-nm laser power.

temperature jump in a long time scale (hundreds of nanoseconds to milliseconds).[46,47] However, the present experimental results are not from the photothermal process. Because the 1064-nm laser photon resonates to the $D_1 \leftarrow D_0$ transition of $Np_2^{\bullet+}$ and only $Np_2^{\bullet+}$ can be excited during the second 1064-nm laser irradiation, the rapid bleaching of $Np_2^{\bullet+}$ at 570 and 1000 nm together with the growth of $Np^{\bullet+}$ at 685 nm (Figure 2A,B,C) correspond to the photodissociation of $Np_2^{\bullet+}$ in the excited D_1 state ($Np_2^{\bullet+}(D_1)$) to give $Np^{\bullet+}$ and Np within the 5-ns laser flash duration (eq 1).

$$Np_2^{\bullet+}(D_0) + h\nu_{1064} \rightarrow Np_2^{\bullet+}(D_1) \rightarrow Np^{\bullet+}(D_0) + Np \quad (1)$$

The plots of $\Delta\Delta OD_{570}$ and $\Delta\Delta OD_{685}$ vs 1064-nm laser power showed the linear lines (Figure 4), indicating that the dissociation of $Np_2^{\bullet+}$ proceeds via one-photon excitation, and that the dissociation yield giving $Np^{\bullet+}$ and Np is 100% yield based on the disappearance of $Np_2^{\bullet+}$. The quantum yield (Φ) of the dissociation of $Np_2^{\bullet+}$ was estimated to be 3.2×10^{-3} from the slope of the linear line in Figure 4. The photon number absorbed by $Np_2^{\bullet+}$ at 1064 nm was measured by using a laser power meter. The concentration of $Np^{\bullet+}$ produced from the dissociation of $Np_2^{\bullet+}$ was calculated to be 4.8×10^{-6} M based on the molar absorption coefficient (ϵ) of 4500 M^{-1} cm^{-1} at 685 nm for $Np^{\bullet+}$ and the 1064-nm laser intensity of 120 mJ flash^{-1}.[31,32]

Following the bleaching of the transient absorption at 570 and 1000 nm, the recovery occurred in the time scale of several tens of nanoseconds. Simultaneously, the 685-nm band decayed in the same time scale. Since the transient absorption bands at 570, 1000, and 685 nm recovered completely, the dimerization of $Np^{\bullet+}$ and Np occurred to give $Np_2^{\bullet+}$ in 100% yield (eq 2).

$$Np^{\bullet+}(D_0) + Np \rightarrow Np_2^{\bullet+}(D_0) \quad (2)$$

Since the Np concentration (1.0×10^{-2} M) was much larger than that of $Np^{\bullet+}$ produced from the photodissociation of $Np_2^{\bullet+}$, the recovery and decay time profiles of the absorption at 570, 1000, and 685 nm, respectively, were well fitted with the pseudo-first-order exponential function as shown in Figure 2 insets, and the recovery and decay rates depended on the Np concentration. The bimolecular rate constant (k_{dim}) of the formation of $Np_2^{\bullet+}$ by the dimerization of $Np^{\bullet+}$ and Np was calculated to be $(1.1 \pm 0.2) \times 10^{10}$ M^{-1} s^{-1} from the slope of the linear plot between the observed rate constants (k_{obs}) of the recovery and decay time profiles and the Np concentration (Figure 5).

The k_{dim} value was found to be almost equal to the diffusion-controlled rate constant in acetonitrile ($k_{diff} = 1.9 \times 10^{10}$ M^{-1} s^{-1}, 25 °C).[48] It is well-known that the dimerization of $Np^{\bullet+}$ and Np occurs at k_{diff} in various solvents.[5,26,30,42] The regeneration of $Np_2^{\bullet+}$ at k_{diff} in the present reaction indicates that the photodissociation of $Np_2^{\bullet+}$ proceeds to give free $Np^{\bullet+}$ and Np in acetonitrile.

Photodissociation and Regeneration of $Np_2^{\bullet+}$ during the Pulse Radiolysis−Laser Flash Photolysis Combined Method. Pulse radiolysis of substrates in chloroalkanes (RCl) has been used as a standard method to generate the substrate radical cations.[39,49−51] $Np^{\bullet+}$ and $Np_2^{\bullet+}$ were produced during the pulse radiolysis of Np (1.0×10^{-2} M) in DCE at room-temperature according to eqs 3−7.

$$RCl \overset{e^-}{\rightsquigarrow} RCl^{\bullet+} + e^-, RCl^* \quad (3)$$

$$RCl + e^- \rightarrow R^\bullet + Cl^- \quad (4)$$

$$RCl^{\bullet+} + Np \rightarrow Np^{\bullet+} + RCl \quad (5)$$

$$Np^{\bullet+} + Np \xrightarrow{k_{dim} = k_{diff}} Np_2^{\bullet+} \quad (6)$$

$$Np^{\bullet+} \text{ (and } Np_2^{\bullet+}) + Cl^- \xrightarrow{k_{neutral}} \text{product} \quad (7)$$

The transient absorption spectra of $Np^{\bullet+}$ and $Np_2^{\bullet+}$ in the visible and near-IR regions in DCE were shown in Figure 6. The absorption band at 700 nm is assigned to $Np^{\bullet+}$.[30,42] The

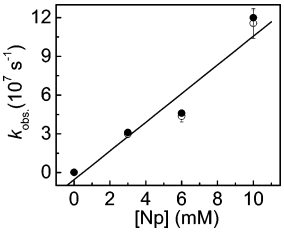

Figure 5. Plots of the observed rate constants (k_{obs}) of the recovery and decay time profiles at 570 and 685 nm (open and solid circles, respectively) during the second 1064-nm laser irradiation vs the Np concentration.

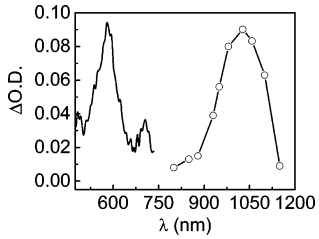

Figure 6. Transient absorption spectrum observed at 20 ns after the 8-ns electron pulse during the pulse radiolysis of Np (1.0×10^{-2} M) in DCE.

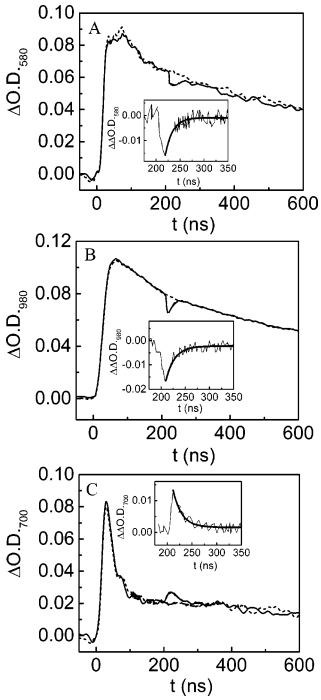

Figure 7. Time profiles of the transient absorption at 580 (A), 980 (B), and 700 nm (C) assigned to $Np_2^{\bullet+}$, $Np_2^{\bullet+}$, and $Np^{\bullet+}$, respectively, during the pulse radiolysis (dotted line) and the pulse radiolysis−laser flash photolysis combined method with the 1064-nm laser flash of 160 mJ $flash^{-1}$ (solid line). The insets show the time profiles of the absorption changes during the second 1064-nm laser irradiation obtained by subtraction of the dotted line from the solid line. The bold solid line in the inset was the fitting curve as the pseudo-first-order exponential function. The delay time of the 1064-nm laser after the electron pulse was 200 ns.

absorption bands around 580 and 1050 nm are assigned to the LE and CR bands of $Np_2^{\bullet+}$, respectively.[27,29,30,32] The absorption peaks of $Np^{\bullet+}$ and $Np_2^{\bullet+}$ in DCE shifted to the longer wavelengths in a few tens of nanometers compared with those in acetonitrile.[39,40,51] Since the decay profile of the 700-nm absorption in Figure 7C was almost the same as the growth profiles of the 580- and 980-nm bands in parts A and B of Figure 7 in the time scale of 5−100 ns, these profiles correspond to the dimerization of $Np^{\bullet+}$ and Np (eq 6). The rate constant was calculated to be $k_{diff} = 7.8 \times 10^9$ M^{-1} s^{-1} in DCE at 25 °C.[48] The decay in the long time scale (>100 ns) at 580, 980, and 700 nm was mainly due to the neutralization of $Np_2^{\bullet+}$ and $Np^{\bullet+}$ with chloride ion (eq 7). Because the equilibrium exists between $Np^{\bullet+}$ and $Np_2^{\bullet+}$, the dacay showed similar behavior for the absorption at 580, 980, and 700 nm.

SCHEME 2: Schematic Diagrams for $Np_2^{\bullet+}(D_0)$, $Np_2^{\bullet+}(D_1)$, $Np^{\bullet+}(D_0)$, and $Np^{\bullet+}(D_1)$[a]

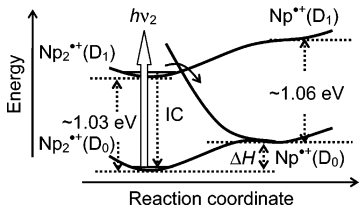

[a] $h\nu_2$ is the second 1064-nm laser flash. IC is the internal conversion. The arrow shows the dissociation of $Np_2^{\bullet+}(D_1)$ to $Np^{\bullet+}(D_0)$ through the crossing of two potential surfaces.

Selective photoexcitation of $Np_2^{\bullet+}$ was carried out in DCE with the pulse radiolysis−laser flash photolysis combined method.[39,40,51] The experimental results observed were similar to those observed during the two-color two-laser flash photolysis of Np in acetonitrile. The bleaching and recovery of the absorption bands of $Np_2^{\bullet+}$ at 580 and 980 nm were observed together with the growth and decay of $Np^{\bullet+}$ at 700 nm during the second 1064-nm laser irradiation as shown in Figure 7. Obviously, the photodissociation and the subsequent regeneration of intermolecular $Np_2^{\bullet+}$ occurred during the 1064-nm laser irradiation of $Np_2^{\bullet+}$. The insets in Figure 7A,B,C show the time profiles of the absorption changes during the second 1064-nm laser irradiation. The rapid bleaching of $Np_2^{\bullet+}$ at 580 and 980 nm as well as the growth of $Np^{\bullet+}$ at 700 nm correspond to the photodissociation of $Np_2^{\bullet+}(D_1)$ to give $Np^{\bullet+}$ and Np within the 5-ns laser flash duration. The recovery of $Np_2^{\bullet+}$ at 580 and 980 nm as well as the decay of $Np^{\bullet+}$ at 700 nm correspond to the dimerization of $Np^{\bullet+}$ and Np to give $Np_2^{\bullet+}$. The k_{dim} of the formation of $Np_2^{\bullet+}$ was calculated to be $(7.7 \pm 0.6) \times 10^9$ M^{-1} s^{-1}, which was nearly equal to $k_{diff} = 7.8 \times 10^9$ M^{-1} s^{-1} in DCE at 25 °C.[48]

Mechanisms of Photodissociation and Regeneration of $Np_2^{\bullet+}$. Because the $-\Delta H$ value for the formation of $Np_2^{\bullet+}$ from the dimerization of $Np^{\bullet+}$ and Np is approximately 50 kJ mol^{-1},[27,31,32] $Np_2^{\bullet+}$ is more stable than $Np^{\bullet+}$ in solution. The dimerization of $Np^{\bullet+}$ and Np occurs at $k_{dim} = k_{diff}$ to give $Np_2^{\bullet+}$. Since the $-\Delta H$ value is approximately equal to half of the energy gap of the CR band,[27,29] irradiation of $Np_2^{\bullet+}(D_0)$ at the CR band with the 1064-nm laser provides enough high energy for the dissociation of $Np_2^{\bullet+}(D_1)$ to give $Np^{\bullet+}(D_1)$ and Np through the crossing of two potential surfaces of $Np_2^{\bullet+}(D_1)$ and $Np^{\bullet+}(D_0)$ as shown in Scheme 2.

The small Φ value indicates that the main deactivation pathway of $Np_2^{\bullet+}(D_1)$ is the internal conversion to $Np_2^{\bullet+}(D_0)$, while the dissociation of $Np_2^{\bullet+}(D_1)$ occurs as a minor pathway. It should be noted that $Np_2^{\bullet+}(D_1)$ cannot dissociate to $Np^{\bullet+}(D_1)$ + Np, since $Np^{\bullet+}(D_1)$ has higher energy than $Np_2^{\bullet+}(D_1)$.[36,43]

As indicated above, the photodissociation of $Np_2^{\bullet+}(D_1)$ and formation of $Np^{\bullet+}(D_0)$ and Np occur within the 5-ns laser flash duration. On the other hand, the formation of free $Np^{\bullet+}(D_0)$ and Np in solution during the photoirradiation of $Np_2^{\bullet+}$ suggests that $Np^{\bullet+}(D_0)$ and Np can escape from the solvent cage before

SCHEME 3: Schematic Diagrams for Photodissociation of $Np_2^{\bullet+}(D_1)$ To Give $Np^{\bullet+}(D_0)$ and Np and Dimerization of $Np^{\bullet+}(D_0)$ and Np To Give $Np_2^{\bullet+}(D_0)$[a]

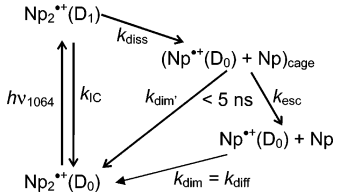

[a] k_{diss} is the rate constant of the dissociation from $Np_2^{\bullet+}(D_1)$ to $Np^{\bullet+}(D_0)$ and Np. k_{IC} is the internal conversion rate constant from $Np_2^{\bullet+}(D_1)$ to $Np_2^{\bullet+}(D_0)$. $k_{dim'}$ is the rate constant of the dimerization of $Np^{\bullet+}(D_0)$ and Np in a cage within 5 ns. k_{esc} is the escape rate constant from $Np^{\bullet+}(D_0)$ and Np in a cage to free $Np^{\bullet+}(D_0)$ and Np. k_{dim} is the rate constant of the dimerization of $Np^{\bullet+}(D_0)$ and Np, which is equal to k_{diff}.

regeneration of $Np_2^{\bullet+}(D_0)$. Therefore, the small Φ value indicates that the rapid regeneration of $Np_2^{\bullet+}$ within a solvent cage is assumed to occur as well as the dissociation of $Np_2^{\bullet+}$ within the 5-ns laser flash duration (Scheme 3). The initial Φ value for the dissociation of $Np_2^{\bullet+}$ into $Np^{\bullet+}$ and Np in a cage may be much larger than the apparent Φ value.

During the 1064-nm irradiation of $Np_2^{\bullet+}(D_0)$, $Np_2^{\bullet+}(D_0)$ is excited to $Np_2^{\bullet+}(D_1)$, from which rapid internal conversion from $Np_2^{\bullet+}(D_1)$ to $Np_2^{\bullet+}(D_0)$ occurs at k_{IC}. $Np_2^{\bullet+}$ partly dissociates to $Np^{\bullet+}(D_0)$ and Np in a cage at k_{diss}, from which $Np^{\bullet+}(D_0)$ and Np escape at k_{esc} to give free $Np^{\bullet+}(D_0)$ and Np. Therefore, the apparent Φ value, $\Phi = [k_{diss}/(k_{diss} + k_{IC})][k_{esc}/(k_{esc} + k_{dim'})] = 0.0032$, was obtained, where k_{diss}, k_{IC}, k_{esc}, and k_{dim} denote the rate constants of the dissociation from $Np_2^{\bullet+}(D_1)$ to $Np^{\bullet+}(D_0)$ and Np, the internal conversion from $Np_2^{\bullet+}(D_1)$ to $Np_2^{\bullet+}(D_0)$, the escape from $Np^{\bullet+}(D_0)$ and Np in a cage to free $Np^{\bullet+}(D_0)$ and Np, and the dimerization of $Np^{\bullet+}(D_0)$ and Np in a cage within 5 ns, respectively. The initial Φ value ($\Phi_{initial} = k_{diss}/(k_{diss} + k_{IC})$) of the dissociation from $Np_2^{\bullet+}(D_1)$ to $Np^{\bullet+}(D_0)$ and Np in a cage may be much larger than the apparent Φ, because k_{dim}' is assumed to be larger than k_{esc}.

Conclusions

Photodissociation and regeneration of $Np_2^{\bullet+}$ were observed during the two-color two-laser flash photolysis and pulse radiolysis−laser flash photolysis. When $Np_2^{\bullet+}$ was excited at the CR band of $Np_2^{\bullet+}$ in the near-IR region with the 1064-nm laser, the bleaching and recovery of the transient absorption at 570 and 1000 nm assigned to $Np_2^{\bullet+}$ were observed together with the growth and decay of the transient absorption at 685 nm assigned to $Np^{\bullet+}$. The bleaching of the transient absorption at 570 and 1000 nm corresponds to the photodissociation of $Np_2^{\bullet+}$ to give $Np^{\bullet+}$ and Np. The growth of the transient absorption at 685 nm corresponds to the generation of $Np^{\bullet+}$ from the dissociation of $Np_2^{\bullet+}$. The bleaching of $Np_2^{\bullet+}$ and growth of $Np^{\bullet+}$ occurred within a 5-ns laser flash duration, suggesting that the photodissociation of $Np_2^{\bullet+}$ occurs to give $Np^{\bullet+}$ and Np within 5 ns. The dissociation and regeneration of $Np_2^{\bullet+}$ occurred in 100% yield. The Φ value of the photodissociation of $Np_2^{\bullet+}$ was estimated to be 3.2×10^{-3} and the regeneration of $Np_2^{\bullet+}$ occurred at the rate constants of $(1.1 \pm 0.2) \times 10^{10}$ and $(7.7 \pm 0.6) \times 10^9$ M^{-1} s^{-1} in acetonitrile and DCE, respectively, which are clearly equal to k_{diff}. The photodissociation mechanism can be explained based on the crossing between two potential surfaces of $Np_2^{\bullet+}(D_1)$ and $Np^{\bullet+}(D_0)$. This is the first example of the photodissociation of $Np_2^{\bullet+}$ to give $Np^{\bullet+}$ and Np and the subsequent regeneration of $Np_2^{\bullet+}$ with the two-color two-laser flash photolysis and pulse radiolysis−laser flash photolysis combined method.

Acknowledgment. The authors wish to thank the people in the Radiation Laboratory, The Institute of Scientific and Industrial Research, Osaka University, for running the linear accelerator. This work has been partly supported by a Grant-in-Aid for Scientific Research (Project 17105005, Priority Area (417), 21st Century COE Research, and others) from the Ministry of Education, Culture, Sports, Science and Technology (MEXT) of the Japanese Government. The authors also thank to JSPS for a fellowship for X.C.

Supporting Information Available: The time profile of the $Np^{\bullet+}$ absorption at 685 nm in the time scale of 5−100 ns after the 355-nm laser irradiation of the mixture of Np and Chl in acetonitrile is shown and analyzed by the formation and decay processes via the electron transfer and dimerization, respectively. This material is available free of charge via the Internet at http://pubs.acs.org.

References and Notes

(1) Kochi, J. K.; Rathore, R.; Le Magueres, P. *J. Org. Chem.* **2000**, *65*, 6826.
(2) Todo, M.; Okamoto, K.; Seki, S.; Tagawa, S. *Chem. Phys. Lett.* **2004**, *399*, 378.
(3) Milosevich, S. A.; Saichek, K.; Hinchey, L.; England, W. B.; Kovacic, P. *J. Am. Chem. Soc.* **1983**, *105*, 1088.
(4) Chandra, A. K.; Bhanuprakash, K.; Bhasu, V. C. J.; Srikanthan, D. *Mol. Phys.* **1984**, *52*, 733.
(5) Kira, A.; Imamura, M. *J. Phys. Chem.* **1979**, *83*, 2267.
(6) Gerson, F.; Kaupp, G.; Ohya-Nishiguchi, H. *Angew. Chem.* **1977**, *89*, 666.
(7) Kawai, K.; Yoshida, H.; Sugimoto, A.; Fujitsuka, M.; Majima, T. *J. Am. Chem. Soc.* **2005**, *127*, 13232.
(8) Kawai, K.; Miyamoto, K.; Tojo, S.; Majima, T. *J. Am. Chem. Soc.* **2003**, *125*, 912.
(9) Hara, M.; Tojo, S.; Kawai, K.; Majima, T. *Phys. Chem. Chem. Phys.* **2004**, *6*, 3215.
(10) Yamamoto, M.; Tsujii, Y.; Tsuchida, A. *Chem. Phys. Lett.* **1989**, *154*, 559.
(11) Tsujii, Y.; Takami, K.; Tsuchida, A.; Ito, S.; Onogi, Y.; Yamamoto, M. *Polym. J.* **1990**, *22*, 319.
(12) Tsujii, Y.; Tsuchida, A.; Yamamoto, M.; Momose, T.; Shida, T. *J. Phys. Chem.* **1991**, *95*, 8635.
(13) Fujitsuka, M.; Samori, S.; Hara, M.; Tojo, S.; Yamashiro, S.; Shinmyozu, T.; Majima, T. *J. Phys. Chem. A* **2005**, *109*, 3531.
(14) Kawai, K.; Yoshida, H.; Takada, T.; Tojo, S.; Majima, T. *J. Phys. Chem. B* **2004**, *108*, 13547.
(15) Kelley, S. O.; Barton, J. K. *Science* **199X**, *283*, 375.
(16) Lewis, F. D.; Liu, X.; Liu, J.; Miller, S. E.; Hayes, R. T.; Wasielewski, M. R. *Nature* **2000**, *406*, 51.
(17) Kawai, K.; Takada, T.; Nagai, T.; Cai, X.; Sugimoto, A.; Fujitsuka, M.; Majima, T. *J. Am. Chem. Soc.* **2003**, *125*, 16198.
(18) Saito, I.; Nakamura, T.; Nakatani, K.; Yoshioka, Y.; Yamaguchi, K.; Sugiyama, H. *J. Am. Chem. Soc.* **1998**, *120*, 12686.
(19) Takada, T.; Kawai, K.; Fujitsuka, M.; Majima, T. *Proc. Natl. Acad. Sci. U.S.A.* **2004**, *101*, 14002.
(20) Lewis, I. C.; Singer, L. S. *J. Chem. Phys.* **1965**, *43*, 2712.
(21) Badger, B.; Brocklehurst, B.; Russell, R. D. *Chem. Phys. Lett.* **1967**, *1*, 122.
(22) Badger, B.; Brocklehurst, B. *Nature* **1968**, *219*, 263.
(23) Badger, B.; Brocklehurst, B. *Trans. Faraday Soc.* **1969**, *65*, 2588.
(24) Badger, B.; Brocklehurst, B. *Trans. Faraday Soc.* **1970**, *66*, 2939.
(25) Shida, T.; Iwata, S. *J. Am. Chem. Soc.* **1973**, *95*, 3473.
(26) Kira, A.; Imamura, M.; Shida, T. *J. Phys. Chem.* **1976**, *80*, 1445.
(27) Inokuchi, Y.; Ohashi, K.; Matsumoto, M.; Nishi, N. *J. Phys. Chem.* **1995**, *99*, 3416.
(28) Hashimoto, S. *Chem. Phys. Lett.* **1996**, *262*, 292.
(29) Tsujii, Y.; Tsuchida, A.; Ito, S.; Yamamoto, M. *Macromolecules* **1991**, *24*, 4061.
(30) Tsuchida, A.; Tsujii, Y.; Ito, S.; Yamamoto, M.; Wada, Y. *J. Phys. Chem.* **1989**, *93*, 1244.
(31) Fushimi, T.; Fujita, Y.; Ohkita, H.; Ito, S. *J. Photochem. Photobiol. A* **2004**, *165*, 69.

(32) Fushimi, T.; Fujita, Y.; Ohkita, H.; Ito, S. *Bull. Chem. Soc. Jpn.* **2004**, *77*, 1443.
(33) Fujiwara, T.; Lim, E. C. *J. Phys. Chem. A* **2003**, *107*, 4381.
(34) Ohkita, H.; Fushimi, T.; Atsumi, K.; Fujita, Y.; Ito, S.; Yamamoto, M. *Chem. Phys. Lett.* **2003**, *374*, 137.
(35) Fushimi, T.; Ohkita, H.; Ito, S.; Yamamoto, M. *Macromolecules* **2002**, *35*, 9523.
(36) Saigusa, H.; Lim, E. C. *J. Phys. Chem.* **1994**, *98*, 13470.
(37) Saigusa, H.; Lim, E. C. *J. Am. Chem. Soc.* **1995**, *117*, 3862.
(38) Cai, X.; Sakamoto, M.; Hara, M.; Tojo, S.; Ouchi, A.; Sugimoto, A.; Kawai, K.; Endo, M.; Fujitsuka, M.; Majima, T. *J. Phys. Chem. A* **2005**, *109*, 3797.
(39) Ishida, A.; Fukui, M.; Ogawa, H.; Tojo, S.; Majima, T.; Takamuku, S. *J. Phys. Chem.* **1995**, *99*, 10808.
(40) Majima, T.; Fukui, M.; Ishida, A.; Takamuku, S. *J. Phys. Chem.* **1996**, *100*, 8913.
(41) Hilinski, E. F.; Milton, S. V.; Rentzepis, P. M. *J. Am. Chem. Soc.* **1983**, *105*, 5193.
(42) Tsuchida, A.; Yamamoto, M.; Nishijima, Y. *J. Phys. Chem.* **1984**, *88*, 5062.
(43) Salama, F.; Allamandola, L. J. *J. Chem. Phys.* **1991**, *94*, 6964.
(44) Andrews, L.; Kelsall, B. J.; Blankenship, T. A. *J. Phys. Chem.* **1982**, *86*, 2916.
(45) Kira, A.; Arai, S.; Imamura, M. *J. Phys. Chem.* **1972**, *76*, 1119.
(46) Hofrichter, J. *Methods Mol. Biol.* **2001**, *168*, 159.
(47) Takamizawa, A.; Kajimoto, S.; Hobley, J.; Hatanaka, K.; Ohta, K.; Fukumura, H. *Phys. Chem. Chem. Phys.* **2003**, *5*, 888.
(48) Murov, S. L.; Carmichael, I.; Hug, G. L. *Handbook of Photochemistry*; Marcel Dekker: New York, 1993.
(49) Burrows, H. D.; Greatorex, D.; Kemp, T. J. *J. Phys. Chem.* **1972**, *76*, 20.
(50) Sujdak, R. J.; Jones, R. L.; Dorfman, L. M. *J. Am. Chem. Soc.* **1976**, *98*, 4875.
(51) Ichinose, N.; Majima, T. *Chem. Phys. Lett.* **2000**, *322*, 15.